

## **Analytical and Experimental Study of Small Droplet Formation in a Pneumatic Drop-on-Demand Generator**

A. Amirzadeh Goghari\* and S. Chandra  
Department of Mechanical and Industrial Engineering  
University of Toronto  
Toronto, ON M5S 3G8 Canada

### **Abstract**

Pneumatic droplet generators operate by applying pressure oscillations to the liquid inside a nozzle, which creates a periodic motion of the free liquid surface. In this work, an upward-shooting pneumatic droplet generator, made of stainless steel tubes and pipe fittings, is described. The main body of the generator consists of a simple stainless steel cross-junction. A cylindrical nozzle is attached to its bottom outlet, and the top port is connected to a gas cylinder through a solenoid valve. The third outlet of the cross-junction is open to the atmosphere through a stainless steel vent tube. When the valve is opened for a short duration, a gas pressure pulse is applied to the liquid. The gas moves back and forth inside the vent tube which sets up alternating negative and positive pressure inside the generator and oscillates the free liquid surface. The gas pressure oscillations were recorded using a dynamic pressure transducer, which is connected to the last port of the cross-junction. During positive pressure, a liquid jet emerges out of the nozzle; its tip becomes unstable, and finally detaches and forms a small droplet. The negative pressure then pulls the remaining liquid back. Photographs of droplets emerging from the droplet generator showed the oscillation of the liquid surface prior to droplet ejection and the time lag between the pressure oscillation and droplet ejection. The time lag increases as liquid viscosity decreases or the nozzle diameter becomes greater. An approximate analytic model of incompressible liquid motion in the nozzle is also studied. The model demonstrates that the motion of the surface is out of phase with the exciting pressure oscillation. It also predicts that maximum liquid velocity is obtained at an intermediate value of viscosity, making it the most favorable for producing liquid droplets. Experiments confirmed that the largest liquid motion was achieved with a mixture of 60 wt% glycerin with water, and droplets the same size as the nozzle diameter could be produced with this mixture, even when droplets were not formed from pure water or glycerin. Varying the duration of the pressure pulse made it possible to produce droplets smaller than the nozzle (approximately 38% the nozzle diameter).

---

### **Introduction**

In many industrial applications such as inkjet printers producing uniform-size liquid droplets is a key element. Similarly, drop-on-demand ejectors are used to deposit electrically conductive polymers to make electronic circuits [1]. They are also used to dispense solder balls on circuit boards [2], deposit droplets of organic liquids in micro-arrays [3] and to make 3D components out of wax and metal [4, 5]. Decreasing the size of droplets has increased the resolution of inkjet printers and reduced the spacing between solder balls on circuit boards. According to conventional analyses of droplet formation from a liquid jet [6], the droplet diameter would be about twice that of the nozzle, so reducing droplet size requires smaller nozzles, which are difficult to manufacture and prone to clogging.

The most common drop-on-demand generator is the piezoelectric ejector, in which the droplet diameter can be varied using voltage pulses with different shapes. Using this generator Riefler and Wriedt [7] produced water droplets a few microns in diameter. Sakai [8] applied a sequence of negative-positive pressure pulses to modulate the droplet diameter. Chen and Basaran [9] produced small water/glycerin droplets using an alternating negative-positive-negative voltage pulse. With the first negative pulse, liquid was drawn back into the nozzle (Fig. 1a). During the subsequent positive pulse, due to viscous effects near the walls, only the central region of the liquid was forced out (Fig. 1b and c). The second negative pulse pulled liquid back into the nozzle, so that a small droplet detached from the tip of the retreating tongue (Fig. 1d). Water/glycerin droplets as small as 65% of the nozzle diameter were also produced using a pneumatic drop-on-demand generator [10], in which applying a gas pulse set up pressure oscillation in the gas above the surface of the liquid, ejecting a droplet through a nozzle. Although small droplets can be produced with both pneumatic and piezoelectric ejectors, the liquid behavior within the generator is not well un-

---

\*Corresponding author

derstood. This paper describes an analytical model to study the formation of small droplets, and for this purpose, a new upward-shooting pneumatic droplet generator was designed and tested, and the model and experimental results were used to determine conditions under which small droplets can be produced.

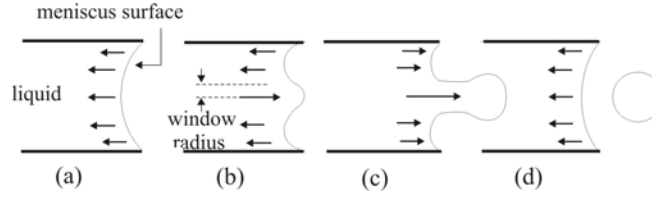


**Figure 1.** Formation of a small droplet

### Experimental Method

The main body of the droplet generator consisted of a stainless steel cross-junction (Model SS-400-4, Swagelok, Solon, OH, USA). Nozzles were press-fit into a nozzle holder, which was filled with liquid at all times by connecting a liquid supply tube to the droplet generator (Fig. 2). Three of the nozzles were commercially available (Swiss Jewel Co., Philadelphia, PA, USA): synthetic sapphire orifices with diameters of 250, 450, and 800  $\mu\text{m}$  (models 2-80-010, -018, and -032). To make a conical shape nozzle a Pyrex tube (OD: 5 mm, thickness: 1 mm) was heated and pulled apart until it broke into two pieces. Each part was ground down until a 200  $\mu\text{m}$  diameter hole was obtained.

The top port of the cross-junction was connected to a nitrogen gas cylinder through a fast response solenoid valve (HSO2L6H50B, Numatics, Highland, MI, USA), which created pressure pulses when activated. One port was open to the atmosphere through a steel tube (length: 50 mm, ID: 4.8 mm) connected to an open valve. The last port was connected to a high-speed dynamic pressure transducer (Type 601B1, Kistler Inst. Corp., New York, USA) to record gas pressure variations. A CCD camera, Sensi Cam High Speed (Type 370 KF, OPTIKON Corp., Kitchener, ON, Canada) with a resolution of 1280x1024 pixels was used to photograph droplets. LabVIEW control software controlled timing of signals for the camera, solenoid valve, and pressure transducer. When the solenoid valve was opened for a preset time, gas flowed into the droplet generator and set up pressure oscillations, which forced liquid out of the nozzle. The liquid jet broke up into droplets due to fluid instability. Then, the gas escaped through the vent tube producing a negative pressure and withdrawing back the remainder of the liquid jet.

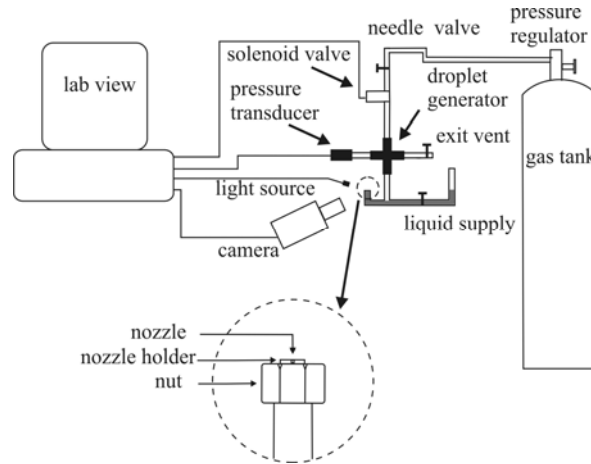


**Figure 2.** Schematic diagram of the experimental apparatus

### Free-surface, oscillating flow in a nozzle

Several analytical models have been developed to describe oscillating incompressible fluid flow, with a free surface, in a nozzle [11, 12]. The model used in this work, in which the oscillating fluid flow takes place in a cylindrical nozzle (Fig. 3) is based on that developed by Shin et al. [12].

A periodically varying pressure  $P_i(t) = Ae^{i\omega t}$  is applied at the nozzle inlet, where  $A$  is the amplitude and  $\omega$  the angular frequency. Neglecting radial pressure gradient and body forces, the continuity and momentum equations are:

$$\frac{\partial u_z}{\partial z} = 0 \quad (1)$$

$$\frac{\partial u_z}{\partial t} = -\frac{1}{\rho} \frac{\partial P}{\partial z} + \nu \left[ \frac{1}{r} \frac{\partial u_z}{\partial r} + \frac{\partial^2 u_z}{\partial r^2} \right]. \quad (2)$$

Neglecting damping effects, the fluid pressure and velocity are assumed to be in the following forms:

$$P(z, t) = P'(z) e^{i\omega t} \quad \text{and} \quad u_z(r, t) = u'_z(r) e^{i\omega t}. \quad (3)$$

Substituting equation (3) into (2) and applying no-slip boundary condition  $u_z(R, t) = 0$  and  $u_z(0, t) = \text{finite}$  gives [12]

$$u'_z(r, t) = \frac{1}{\rho i \omega} \frac{\partial P'(z)}{\partial z} \left[ \frac{J_0(kr)}{J_0(kR)} - 1 \right] e^{i\omega t}, \quad (4)$$

where  $k = \sqrt{-i\omega/\nu}$  and  $J_0$  is the Bessel function of the first kind. The pressure function  $P'(z)$  can be obtained by substituting equation (4) into equation (1); hence, the pressure and velocity distributions will be:

$$P(z, t) = (c_1 z + c_2) e^{i\omega t} \quad \text{and} \quad u'_z(r, t) = \frac{c_1}{\rho i \omega} \left[ \frac{J_0(kr)}{J_0(kR)} - 1 \right] e^{i\omega t}, \quad (5)$$

where  $c_2$  and  $c_1$  can be obtained using the upstream  $P(0, t) = P_i(t)$  and downstream pressure boundary conditions, respectively. Since the axial velocity is assumed to be the dominant factor in determining the meniscus shape, the location of the free surface can be approximated as follows:

$$u_z = \frac{\partial \eta}{\partial t} \quad \text{or} \quad \eta(r, t) = \frac{-c_1}{\rho \omega^2} \left[ \frac{J_0(kr)}{J_0(kR)} - 1 \right] e^{i\omega t} \quad (6)$$

The overall pressure difference at the liquid-air interface can be obtained using axial force balance at the nozzle exit. If non-linear effects are neglected at the onset of meniscus displacement, the downstream pressure will be

$$P(L, t) = \frac{1}{\pi R^2} \int_0^R \sigma \left[ \frac{\partial^2 \eta}{\partial r^2} + \frac{1}{r} \frac{\partial \eta}{\partial r} \right] 2\pi r dr, \quad (7)$$

where  $\sigma$  is the surface tension; hence,  $c_1$  can be obtained by substituting for  $P$  and  $\eta$ .

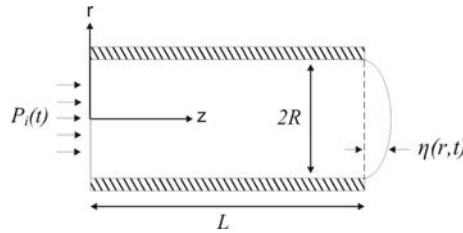


**Figure 3.** Nozzle cross-section

The gas pressure oscillation inside the generator was modeled using the peak pressure from experiments as the amplitude. The angular frequency  $\omega = 2\pi f$  was calculated using the measured frequency from experiments, 294 Hz. Physical properties of water/glycerin mixtures at 25°C [13] were used in the analysis. Fig. 4 shows the gas pressure variation and the meniscus displacement for three different mixtures in a 250  $\mu\text{m}$  diameter nozzle. There is a phase shift between the pressure and the response of the liquid surface: increasing viscosity reduces the phase shift. Similar results were obtained using 450 and 800  $\mu\text{m}$  diameter nozzles. Reducing nozzle diameter increases the resistance

to liquid flow through it and has an effect similar to increasing viscosity: it reduces both the phase lag and amplitude of meniscus oscillations. Maximum velocity is obtained at an intermediate viscosity (60wt% glycerin mixture).

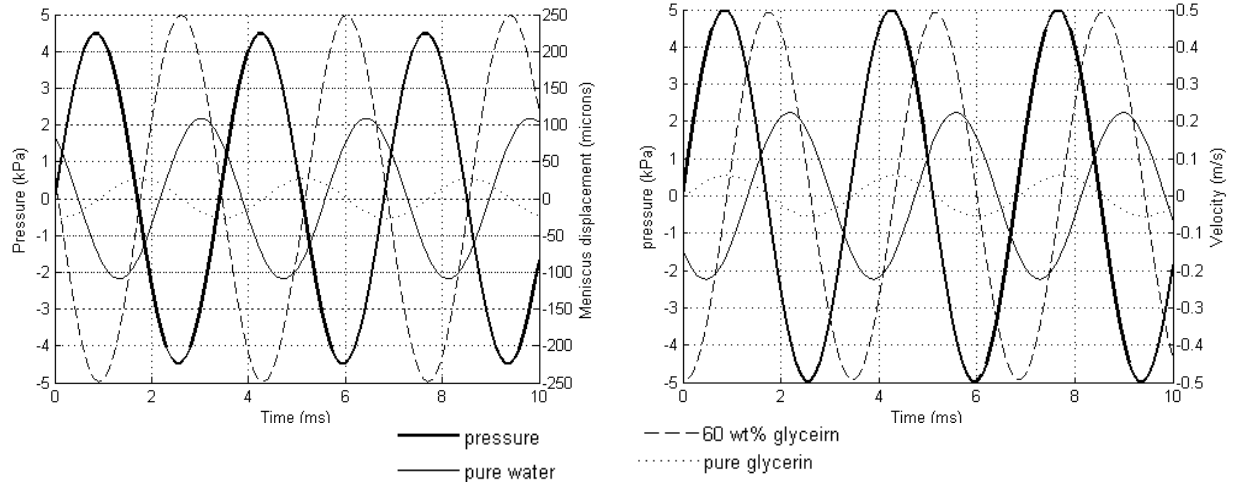
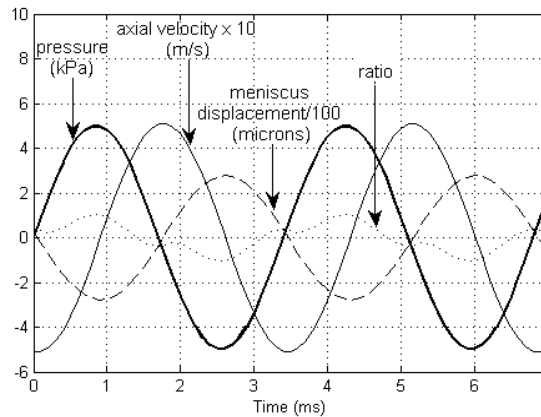


**Figure 4.** Gas pressure variation, meniscus displacement, and axial velocity variation,  $2R = 250 \mu\text{m}$ ,  $f = 294 \text{ Hz}$

If the rate of change of kinetic energy to the rate of change of surface energy in a certain circular window of radius  $r_w$  (Fig. 1) becomes greater than unity, this region of the meniscus will start bulging out, grow longer, and its tip will detach when the meniscus withdraws. This ratio  $\xi$  is given by [12]

$$\xi = \frac{dK}{dS} = \frac{\rho u_z^3}{2\sigma \frac{\partial \eta}{\partial r} \frac{\partial u_z}{\partial r}} \sqrt{1 + \left( \frac{\partial \eta}{\partial r} \right)^2}. \quad (8)$$

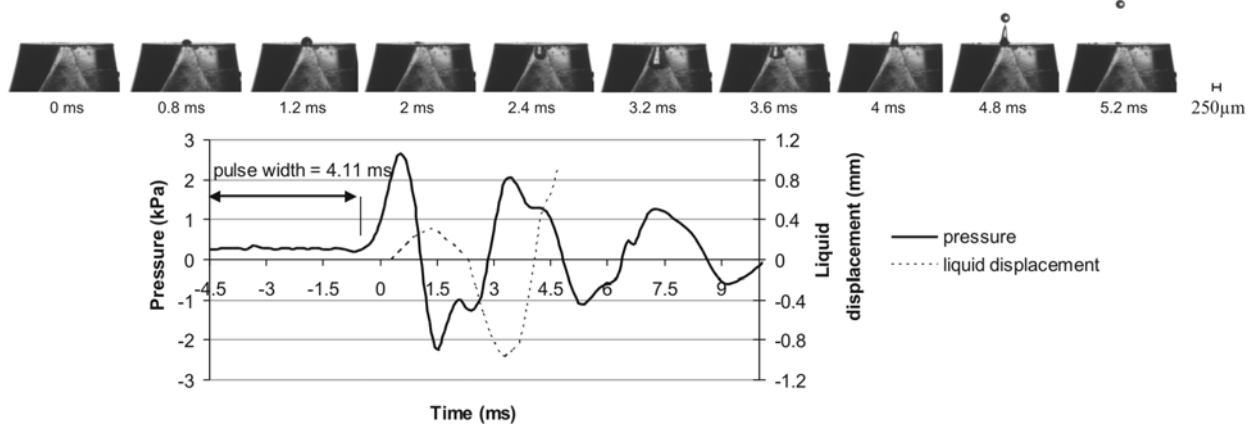
The model predicted the largest window radius  $r_w$  for which  $\xi$  reached a value of 1 at some time over the pressure cycle. The mixture with 60 wt% glycerin had the largest window radius ( $r_w = 23 \mu\text{m}$ ) compared to that of pure water ( $r_w = 16 \mu\text{m}$ ) and glycerin ( $r_w = 8 \mu\text{m}$ ), because it had the highest velocity. Droplet formation can be understood in terms of the variation of  $\xi$  relative to the meniscus motion. Fig. 5 shows the pressure, velocity, meniscus motion, and ratio variation for the 60 wt % glycerin mixture in a  $250 \mu\text{m}$  nozzle. The axial velocity becomes positive at  $t = 0.9 \text{ ms}$  and, at this time, the meniscus starts moving forward from its minimum point. The ratio  $\xi$ , calculated with a window radius of  $r_w = 23 \mu\text{m}$ , becomes unity at  $t = 0.9 \text{ ms}$ . At this instant, a liquid jet of radius  $r_w$  breaks through the meniscus surface and begins to grow. At  $t = 2.6 \text{ ms}$  the displacement of the meniscus reaches its peak while the velocity becomes negative: a droplet would be expected to detach from the liquid tip at this time. High and low viscosity liquids both have smaller meniscus displacements (Fig. 4), so no droplets will detach.



**Figure 5.** Pressure, velocity, meniscus motion, and ratio variations for a 60 wt% glycerin mixture,  $2R = 250 \mu\text{m}$

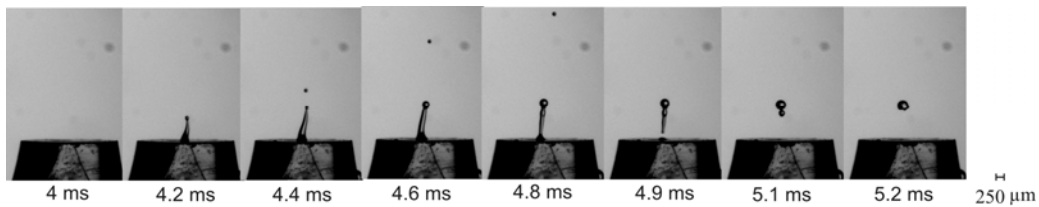
## Results and Discussion

Figure 6 shows a droplet of a 60 wt% glycerin mixture emerging from a 200  $\mu\text{m}$  conical shape nozzle and the corresponding pressure variation. Time  $t=0$  corresponds to the first image. Liquid starts emerging from the nozzle at approximately  $t=0.8$  ms and reaches a maximum height at  $t=1.2$  ms, but the pressure has become negative at this time. This time delay is similar to that predicted in Fig. 5. The liquid withdraws into the nozzle from  $t=2.4$  to 3.6 ms. The pressure then becomes positive, and the liquid is driven out far enough for the tip to become unstable and detach ( $t=4.8$  ms). The emerging droplet has approximately the same diameter as the nozzle. When the pulse width was increased to 4.2 ms, the length of the liquid jet was longer, and a small droplet, approximately 75  $\mu\text{m}$  in diameter, broke off first at  $t=4.4$  ms (Fig. 7). Then, at  $t=4.9$  ms, the ligament, which was not possible to suppress, broke off.



**Figure 6.** Formation of a single droplet using a conical shape nozzle 200  $\mu\text{m}$  in diameter, Liquid: mixture with 60 wt% glycerin, Supply pressure: 207 kPa, Pulse width: 4.11 ms, Exit vent: 5 cm long tube connected to an open valve

Effect of liquid viscosity was studied using sapphire nozzles with a cylindrical profile similar to that used in the analytical model. Fig. 8 shows the pressure variation and liquid jet height for different liquids. The jet height was largest for the 60 wt% glycerin mixture, as predicted by the model (Fig. 4). The movement of the liquid was out of phase with the pressure pulse, with pure glycerin having the smallest time lag as well as the least amplitude as was previously observed in Fig. 4. The liquid withdrew into the nozzle as the pressure became negative. Increasing the pressure pulse width to 4.61 ms increased the first peak pressure from 3.5 to 3.8 kPa and increased the amplitude of the meniscus motion sufficiently, so that the 60wt% mixture droplet detached from the nozzle (Fig. 9). Liquid jets of pure water and glycerin were not as long and withdrew without droplet formation.



**Figure 7.** Formation of a small droplet followed by a larger droplet, Nozzle diameter: 200  $\mu\text{m}$ , Liquid: 60 wt% glycerin mixture, Supply pressure: 207 kPa, Pulse width: 4.2 ms, Exit vent: 5 cm long tube attached to an open valve

When the nozzle diameter was increased to 450  $\mu\text{m}$ , while the pulse width was maintained at 4.4 ms, the amplitude of the meniscus motion increased. The model had predicted the increased displacement for larger nozzle size. However, the jet diameter also increased and the jet length was still not sufficient to allow a droplet to detach.

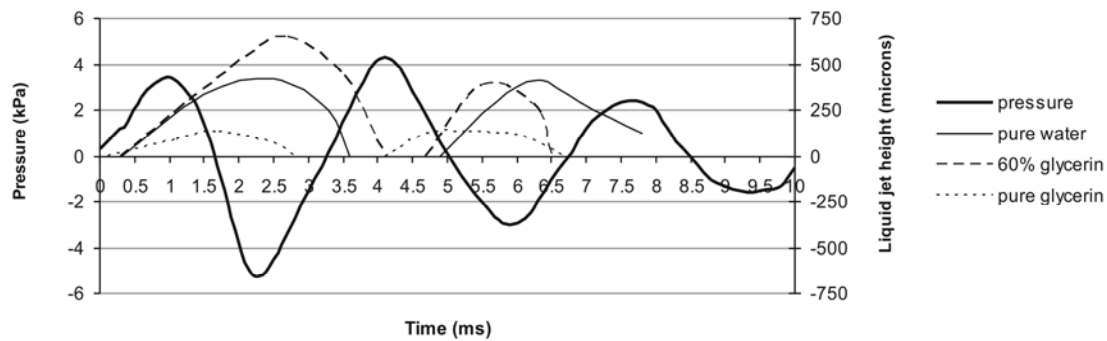


**Figure 8.** Meniscus displacement, Nozzle diameter: 250  $\mu\text{m}$ , Supply pressure: 207 kPa, Pulse width: 4.4 ms, Exit vent: 5 cm long tube connected to an open valve

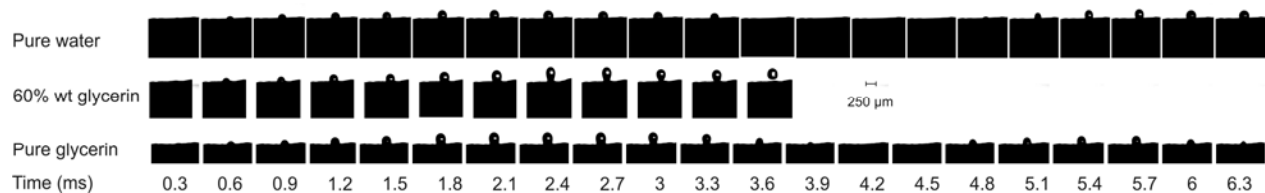


**Figure 9.** Liquid jet emerging from a 250  $\mu\text{m}$  diameter nozzle when the pulse width was set to 4.61 ms, Supply pressure: 207 kPa, Exit vent: 5 cm long tube connected to an open valve

### Summary and Conclusions

Pneumatic droplet generators operate by applying pressure oscillations to the liquid inside the nozzle, which excite a periodic motion of the free liquid surface. An analytic model of incompressible liquid motion in the nozzle shows that the motion of the surface is out of phase with the pressure oscillation. The time lag increases as liquid viscosity decreases or the nozzle diameter increases. The maximum liquid velocity is attained at an intermediate value of viscosity, making it the most favorable for producing liquid droplets. Photographs of emerging droplets showed the oscillation of the liquid surface prior to droplet ejection and the time lag between the pressure oscillation and meniscus motion. Experiments confirmed that the largest liquid motion was achieved with a 60 wt% glycerin mixture. Droplets could be produced with this mixture, even when droplets were not formed from pure water or glycerin. Varying the pulse width of the applied pressure made it possible to produce droplets smaller than the nozzle diameter.

### References

1. De Gans, B.-J., Duineveld, P. C., and Shubert, U.S., *Advanced Materials*, 16: 203-213 (2004).
2. Orme, M., and Smith, R. F., *ASME Journal of Manufacturing Science and Engineering*, 122: 484-493 (2000).
3. Shena, M., Heller, R. A., Theriault, T.P., Konrad, K., Lachenmeier, E., and Davis, R.W., *Trends in Biotechnology*, 16: 301-306 (1998).
4. Gao, F., and Sonin, A., *Proceedings of the Royal Society of London Series A*, 444: 533-553 (1994).
5. Fang, M., Chandra, S., Park, C.B., *Journal of Rapid Prototyping*, 14: 44-52 (2008).
6. Rayleigh, F. R. S., *Proceedings of the London Mathematical Society*, 10: 4-13 (1878).
7. Riefler, N., and Wriedt, T., *Particle and Particle Systems Characterization*, 25: 176-182 (2008).
8. Sakai, S., *Proceedings of IS & T NIP 16: International Conference on Digital Printing Technologies* (2000).
9. Chen, A.U., and Basaran, O.A., *Physics of Fluids*, 14: L1-L4 (2002).
10. Amirzadeh Goghari, A., and Chandra, S., *Experiments in Fluids*, 44: 105-114 (2008).
11. Hart, V.G., and Shi, J., *International Journal of Engineering Science*, 33: 1121-1138 (1995).
12. Shin, D.Y., Grassia, P., and Derby, B., *Transactions of the ASME Journal of Fluids Engineering*, 127: 98-109 (2005).
13. Timmermans, J., *The physico-chemical constants of binary systems in concentrated solutions*, New York: Interscience Publishers 4: 252 (1960).